



SCUOLA  
ALTI STUDI  
LUCCA

Scuola IMT Alti Studi Lucca

## How do children fall asleep? A high-density EEG study of slow waves in the transition from wake to sleep

Questa è la versione sottoposta a revisione paritaria (postprint) della seguente opera:

*Original*

How do children fall asleep? A high-density EEG study of slow waves in the transition from wake to sleep / Spiess, Mathilde; Bernardi, Giulio; Kurth, Salome; Ringli, Maya; Wehrle, Flavia M.; Jenni, Oskar G.; Huber, Reto; Siclari, Francesca. - In: NEUROIMAGE. - ISSN 1053-8119. - 178:(2018), pp. 23-35. [10.1016/j.neuroimage.2018.05.024]

*Availability:*

This version is available at: 20.500.11771/11701

*Publisher:*

*Published*

DOI:10.1016/j.neuroimage.2018.05.024

*Terms of use:*

This publication is made accessible in accordance with the terms for deposit in the institutional repository, as defined by the IMT School for Advanced Studies Lucca's Open Access Policy. ([https://library.imtlucca.it/sites/default/files/regolamento-policy-open-access-imtlib\\_0.pdf](https://library.imtlucca.it/sites/default/files/regolamento-policy-open-access-imtlib_0.pdf)).

Si prega di consultare le pagine informative dell'editore relative alle politiche di autoarchiviazione.

(Article begins on next page)

See discussions, stats, and author profiles for this publication at: <https://www.researchgate.net/publication/325120129>

# How do children fall asleep? A high-density EEG study of slow waves in the transition from wake to sleep

Article in *NeuroImage* · May 2018

DOI: 10.1016/j.neuroimage.2018.05.024

CITATIONS

4

READS

180

8 authors, including:



**Mathilde Spiess**

University of Zurich

1 PUBLICATION 4 CITATIONS

SEE PROFILE



**Giulio Bernardi**

IMT School for Advanced Studies Lucca

35 PUBLICATIONS 361 CITATIONS

SEE PROFILE



**Salome Kurth**

University of Zurich

45 PUBLICATIONS 881 CITATIONS

SEE PROFILE



**Flavia Wehrle**

University Children's Hospital Zurich

9 PUBLICATIONS 74 CITATIONS

SEE PROFILE

Some of the authors of this publication are also working on these related projects:



Functional and Anatomical basis of visuo-spatial processing [View project](#)



Zurich Longitudinal Studies: Trajectories to Healthy Aging [View project](#)

## **How do children fall asleep?**

### **A high-density EEG study of slow waves in the transition from wake to sleep**

Mathilde Spiess<sup>1,2\*</sup>, Giulio Bernardi<sup>2,3\*</sup>, Salome Kurth<sup>4</sup>, Maya Ringli<sup>1</sup>, Flavia M. Wehrle<sup>1</sup>, Oskar G. Jenni<sup>1</sup>, Reto Huber<sup>1,5\*\*</sup>, Francesca Siclari<sup>2\*\*</sup>

<sup>1</sup> Child Development Center, University Children's Hospital Zurich, Zurich, Switzerland

<sup>2</sup> Center for Investigation and Research on Sleep, Lausanne University Hospital, Lausanne, Switzerland

<sup>3</sup> MoMiLab Unit, IMT School for Advanced Studies Lucca, Lucca, Italy

<sup>4</sup> Division of Pulmonology, University Hospital Zurich, Zurich, Switzerland

<sup>5</sup> Department of Child and Adolescent Psychiatry and Psychotherapy, Psychiatric Hospital Zurich, Zurich, Switzerland

\* these authors contributed equally to this work

\*\* these authors contributed equally to this work

Correspondence should be addressed to:

Reto Huber (reto.huber@kispi.uzh.ch) or Francesca Siclari (francesca.siclari@chuv.ch)

Word count: abstract 268 words, discussion 2326 words

## **Abstract**

*Introduction:* Slow waves, the hallmarks of non-rapid eye-movement (NREM) sleep, are thought to reflect maturational changes that occur in the cerebral cortex throughout childhood and adolescence. Recent work in adults has revealed evidence for two distinct synchronization processes involved in the generation of slow waves, which sequentially come into play in the transition to sleep. In order to understand how these two processes are affected by developmental changes, we compared slow waves between children and young adults in the falling asleep period.

*Methods:* The sleep onset period (starting 30s before end of alpha activity and ending at the first slow wave sequence) was extracted from 72 sleep onset high-density EEG recordings (128 electrodes) of 49 healthy subjects (age 8-25). Using an automatic slow wave detection algorithm, the number, amplitude and slope of slow waves were analyzed and compared between age groups.

*Results:* Slow wave number and amplitude increased linearly in the falling asleep period in children (age 8-11), while in young adults (age 20-25), isolated high-amplitude slow waves (type I) dominated initially and numerous smaller slow waves (type II) with progressively increasing amplitude occurred later. Compared to young adults, children displayed faster increases in slow wave amplitude and number across the falling asleep period in central and posterior brain regions, respectively, and also showed larger slow waves during wakefulness immediately prior to sleep.

*Conclusions:* Children do not display the two temporally dissociated slow wave synchronization processes in the falling asleep period observed in adults, suggesting that maturational factors underlie the temporal segregation of these two processes. Our findings provide novel perspectives for studying how sleep-related behaviors and dreaming differ between children and adults.

## Introduction

During the transition to sleep, consciousness and brain activity undergo remarkable changes within a short time: the thought-like mental activity of wakefulness gives way to hypnagogic hallucinations in light sleep, before consciousness tends to fade during slow wave sleep early in the night (1). Simultaneously, the fast, low-amplitude desynchronized EEG activity of wake is replaced by high-amplitude slow waves and spindles during sleep. It is now well established that the transition to sleep is not a spatially and temporally uniform process, as previously assumed (2). Instead, recent studies have revealed predictable sequences of regional EEG changes that occur in the transition to sleep. At the subcortical level, the hippocampus consistently displays sleep spindles several minutes before neocortical regions, where these events appear with increasing delays along the cortical antero-posterior axis (3). This differential occurrence of spindles across different cortical regions fits with the observation that the thalamus undergoes deactivation before neocortical areas (4) during the transition to sleep. Moreover, slow wave activity (SWA, the EEG signal power in the 0.5 to 4.0 Hz range) typically displays an anterior-posterior gradient at sleep onset in adults, appearing first in fronto-central regions (5), and only later in posterior brain areas. Supporting such a temporal segregation of cortical regional features of sleep, a recent study provided evidence for two types of slow waves with different characteristics and spatial distributions that are presumably generated by two distinct synchronization processes that sequentially come into play during the transition to sleep (6): a likely subcortico-cortical, arousal-related synchronization process (synchronization process I) generating large, steep and widespread fronto-central slow waves (type I slow waves) that predominate early in the falling asleep period, and a probably cortico-cortical synchronization process (synchronization process II) generating smaller, shallower and more circumscribed slow waves (type II slow waves) that become the predominant feature towards stable sleep, e.g. N3 sleep. A follow-up study showed that slow waves with 'type I' and 'type II' characteristics also co-exist in stable sleep and show opposite changes in the course of a night of sleep (25).

EEG slow waves of sleep occur when thalamocortical neurons become bistable and undergo a slow oscillation between two states: a hyperpolarized ‘down-state’ characterized by neuronal silence (‘off-state’), and a depolarized ‘up-state’ during which neurons fire (‘on-state’) (7). At a global level, slow waves are regulated by a homeostatic process: they increase with time spent awake and decrease across successive NREM sleep cycles in the course of the night (8). At the local level, slow waves are regulated as a function of prior experience and learning (9-11). A visuomotor learning task involving the right parietal area, for instance, leads to an increase in SWA over this brain region during subsequent sleep, while arm immobilization for 12h during daytime produces a decrease in SWA over the contralateral sensorimotor cortex (9, 10). In addition and importantly for our purposes, slow waves also undergo major quantitative and regional changes during development. SWA has been shown to follow a trajectory resembling an inverted U-shape: it increases progressively in early childhood before it declines during adolescence (12-17). Further, the location of maximal SWA gradually shifts from posterior to anterior brain regions during this time (17). Neuroimaging studies have shown that SWA changes are paralleled by structural brain modifications: decreases in cortical thickness follow a similar inverted U-shape during development (18), and regional decreases in grey matter volume during adolescence correlate with SWA decreases (19). Finally, local SWA changes have been shown to be related to the acquisition of regionally specific skills (17, 20). Taken together, these findings have led to the hypothesis that SWA reflects synaptic changes that ultimately account for the benefits of sleep on learning and memory consolidation (21). The nature of synaptic processes underlying SWA changes during development and in particular the drop in SWA during adolescence have been suggested to include synaptic pruning (12, 16) and refinement, i.e. a reorganization of connections without significant change in their number or strength (22) (23).

In the present study we asked whether children, similarly to adults, show evidence for the two temporally dissociated synchronization processes at sleep onset. We hypothesized that if this was the case, only type II slow waves, likely resulting from a cortico-cortical synchronization process would show clear regional developmental changes in relation

with cortical plasticity, while type I slow waves, which are likely related to a subcortico-cortical synchronization process that is dependent on arousal systems, would not.

For optimal comparability with our previous study performed in the adult population, we applied the same criteria to define the falling asleep period (6). More specifically, we analyzed the time period ranging from the end of alpha activity to the first slow wave sequence (generally close to the transition between N2 and N3), and analyzed changes in slow wave parameters over 10 time segments of equal length, using an automatic slow wave detection algorithm. We decided to use this relatively long time period to ensure that the entirety of the spatiotemporal changes that occur in the falling asleep period were included. This approach assumes that falling asleep is a process that occurs regardless of its duration and has the advantage that it can be applied to falling asleep periods of different lengths. We then examined how time courses and spatial distributions of slow waves changed with age, by studying 49 healthy subjects aged 8-25.

## **Methods**

### *Participants*

Overnight high density (hd) EEG recordings (128 electrodes; Electrical Geodesics, Inc., Eugene, OR) of 73 healthy subjects (range 8.7-28.4 years; 49 males, 24 females; 1-2 nights per subject; 122 nights in total) were selected within the age range 8-30 years from the database of recordings collected between 2008 and 2016 in three different studies (17, 24, 25) at the Sleep Laboratory of the University Children's Hospital Zürich (Zürich, Switzerland).

After excluding recordings because of artifacts and non-continuous falling asleep periods (see below), recordings of 49 subjects (range: 8-25 years; 19 females, 30 males; 1-2 nights per subject; 26 subjects with one, 23 subjects with two recording nights; 72 nights in total) were ultimately retained (Fig. 1, see Supplementary Text for details on the studies from which participants were included). Group-level comparisons were carried

out in 32 of these 49 subjects, including the 16 youngest subjects (age 8.7-11.8 yrs, mean  $10.4 \pm 1.0$  yrs, 8 females, ‘children’) and the 16 oldest subjects (age 20.1-25.1 yrs, mean  $22.8 \pm 1.9$  yrs, 6 females, ‘young-adults’) (see *Statistical analyses* section for details). The number of subjects for whom data of two nights (instead of one) was available was similar for children (N=6; 37.5%) and young adults (N=7; 43.8%). For correlation analyses presented in supplementary figures, all 49 subjects were included. Participants had been screened for health problems and time zone travels by telephone and questionnaires (17, 20). Written consent was obtained from participants aged 18 or older or from the parents of individuals < 18 years. Oral consent was also obtained from minors. The procedures were approved by the local ethics committee and in accordance with the Declaration of Helsinki. Analyses of sleep data of 60 of the initial 73 subjects, but not of the falling asleep period, have been previously reported (17, 20).

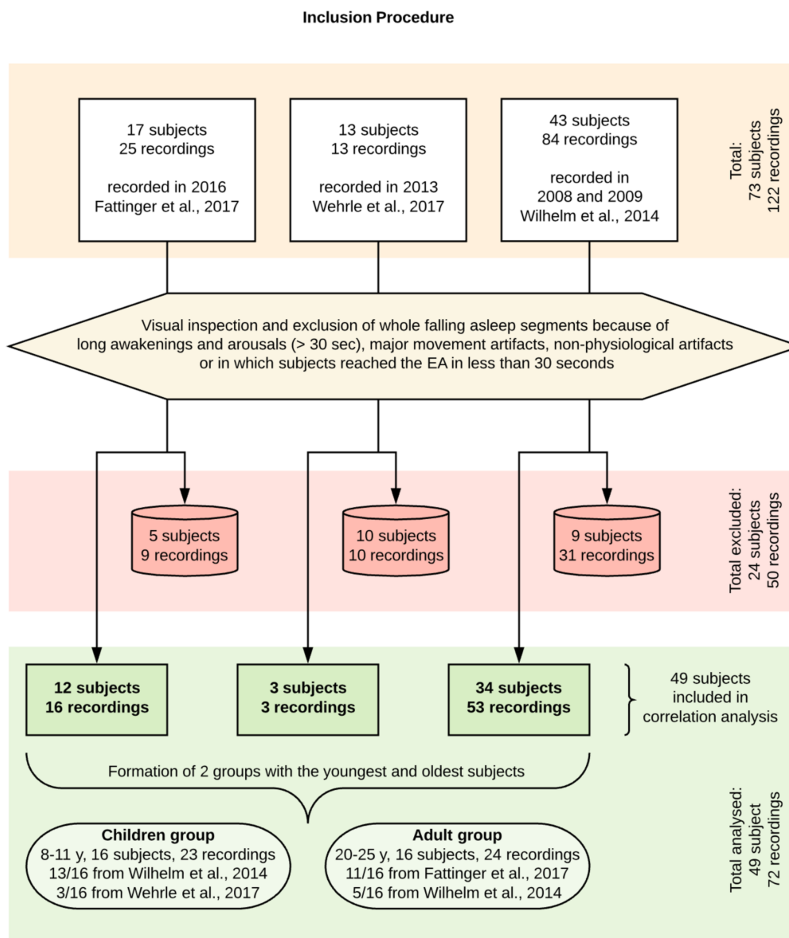


Fig. 1. Inclusion procedure.

### *Recordings*

Participants went to bed at their usual bedtime. A regular sleep schedule approximately one week (range 4-8 days) prior the recording was imposed and controlled with actigraphy and diaries (Actiwatch Type AWL from Cambridge Neurotechnology, CamNtech, Cambridge, UK). Alcohol and drugs/medications were prohibited 48h before the night recording. The EEG signal was acquired in vertex reference, with a sampling frequency of 500 Hz. A 0.5-45 Hz band-pass filter was applied off-line.

### *Definition of the falling asleep period*

EEG recordings were visually inspected by using a selection of 8 electrodes (F3/F4, C3/C4, P3/P4, O1/O2) referenced to the contralateral mastoid channel. Two events, the end of alpha activity (EA) and the first slow wave sequence (FSS), were marked and used to define the beginning and the end of the falling-asleep period, respectively (6). EA was defined as the moment when continuous alpha activity characteristic of wakefulness was replaced by the high-frequency, low-voltage activity typical of stage N1 (26). When alpha activity dropped out intermittently, the end of the last 'alpha burst' was marked as EA. The FSS was defined as the first slow wave burst in the falling-asleep period consisting of more than two successive slow waves in the same derivation (negative half-wave duration  $> 0.5$  sec and peak-to-peak amplitude  $> 75$   $\mu$ V for each slow wave (26)) that were not followed by an arousal. The FSS generally appeared at the transition between stage N2 and N3. We chose this relatively long time period as opposed to one particular event (i.e., the first sleep spindle) to define the falling asleep period in order to capture the process in its entirety. Indeed, the falling asleep process is likely to be a gradual phenomenon, with the majority of behavioral, EEG and physiological changes characteristic of sleep having occurred by the end of stage N2 (27). Falling asleep segments (FASs) containing long awakenings and arousals ( $> 30$  sec), major movement artifacts, non-physiological artifacts (e.g., due to an impedance check) or in which subjects reached the EA in less than 30 seconds were excluded from subsequent analysis. Application of these criteria led to the exclusion of 24 subjects (Fig. 1). This stringent selection allowed us to guarantee the continuity of the falling asleep segments, without

discarding parts with arousal-related muscular artifacts. This was necessary to compare falling asleep segments of different lengths ( $14.3 \pm 4.7$  min (mean  $\pm$  SD), range 3.2-30.7 min) (6). The EEG signal corresponding to each FAS was extracted, including 30 sec before the EA and 30 sec following the FSS.

### *Preprocessing of the EEG signal*

Channels with artifacts were rejected based on the following criteria: i) impedance at recording greater than 50 k $\Omega$ , ii) presence of major artifacts detected through a semi-automated procedure based on changes in power values within delta and beta frequency bands (17), iii) identification of artifacts during visual inspection. Independent Component Analysis (ICA) was performed for each FAS to reduce ocular, muscular, and electrocardiograph artifacts using EEGLAB routines (28). Principal Component Analysis (PCA; 50% dimensionality reduction) was performed before ICA in order to increase the stability of ICA results in relatively short data segments. Only ICA components with specific activity patterns and component maps characteristic of artifactual activity were removed. On average,  $23.3 \pm 7.1$  % of all components were kept across all subjects;  $23.7 \pm 6.0\%$  in the children group (age 8-11) and  $26.7 \pm 8.0\%$  in the adult group (age 20-25) ( $p = 0.911$ ;  $t_{(30)} = -0.112$ ). The removal of a relatively high proportion of ICA components was necessary given that we wanted to preserve the continuity of the signal and could not discard entire artifactual EEG segments. Finally, rejected channels were replaced with data interpolated from nearby channels using spherical splines. After excluding ‘external’ electrodes located on the neck/face region (which commonly display muscular artifacts), a total of 99 ‘internal’ electrodes were ultimately analyzed.

### *Data analysis*

Each FAS, starting from the EA, was divided into 10 time epochs of equal length. This procedure allows to compare FASs of different durations (6). The signal corresponding to the 30 sec before the EA (i.e., wakefulness immediately prior to sleep), was analyzed separately. This time period was present in all subjects and is typically characterized by quiet waking. To better characterize regional changes in the course of the falling-asleep period, four regions of interest (ROIs) were defined: medial anterior, medial posterior,

lateral (left/right) anterior, and lateral (left/right) posterior brain areas (see Fig. 2A). To determine how slow wave properties changed throughout the course of the 10 time epochs, we computed average values of the parameters of interest between homologous time epochs of different FASs for each channel. In order to also take into account the temporal dimension of potential changes, additional analyses were performed by evaluating the magnitude of variations in slow wave parameters over absolute time ('speed of changes'). More specifically, we divided each wake-sleep transition in 1-min epochs (instead of 10 epochs of equal length) and determined the slope of the variation using least square linear regression. For ROI-based analyses, mean values were calculated across channels belonging to the same ROIs.

#### *Slow wave detection*

The detection of individual slow waves was performed as previously described (6, 29). Specifically, the signal of each channel was referenced to the average of the two mastoid electrodes, down-sampled to 128 Hz and band-pass filtered (0.5-4.0 Hz, stop-band at 0.1 and 10 Hz) before an automatic detection algorithm based on signal zero-crossings (29) was applied. To exclude small baseline fluctuations from the analyses and for consistency with our previous work (6), only slow waves with a duration of 0.25-1.0 sec between consecutive zero crossings and a negative-peak amplitude greater than 40  $\mu\text{V}$  (arbitrary threshold) were considered. For all detected slow waves, the following parameters were analyzed: density (number of slow waves per minute), maximum negative amplitude (in  $\mu\text{V}$ ) and slope (i.e., between the first zero crossing and the negative peak, in  $\mu\text{V}/\text{s}$ ). The maximum negative amplitude was chosen as it most accurately reflects the downstate that characterizes the cortical slow oscillation (7). To better characterize potential changes in slow wave properties from the beginning to the end of the wake-sleep transition, direct comparisons were performed between early (2-3) and late (8-9) epochs of the FAS (6). These epochs were considered to be representative for type I and type II slow waves, respectively (6).

### *Brain activity in wakefulness immediately prior to sleep*

The signal of each channel was re-referenced to the average of the 99 included electrodes. Power spectral density (PSD) estimates were computed using the Welch's method in 2-sec Hamming windows (0.5 Hz bin resolution). Since previous studies have shown that low-frequency oscillations may reflect the level of sleep pressure, the analysis focused on the following EEG bands: delta (1.0-4.0 Hz), theta (5.0-8.0 Hz), and alpha (8.0-12 Hz). PSD values were integrated within each band and averaged across 2-sec windows of the pre-sleep period. Given that in both animals and humans, slow waves have been shown to occur not only during sleep, but also during wakefulness, especially under sleep deprivation (30-32), the same slow wave detection algorithm described above was also used to further characterize properties of low-frequency oscillations in the pre-sleep period. Because during wakefulness, low-frequency waves are typically smaller and more localized than in sleep (31), the 40 $\mu$ V amplitude threshold was not applied to the signal acquired during wakefulness immediately prior to sleep.

### *Statistical analyses*

In order to identify potential age-dependent changes involving the wake-sleep transition, both correlation analyses and direct group contrasts were performed. Specifically, correlation analyses with the participants' age were performed by including all subjects (N=49) and by using the Pearson's correlation coefficient. Unless specified otherwise, group-level contrasts were performed by comparing the 16 youngest (age 8-11, 'children') with the 16 oldest subjects (age 20-25 yrs, 'young-adults') with unpaired t-tests. In these analyses, an iterative randomization procedure was used to control for inter-night variability. Specifically, for each of the 1,000 iterations, data from a single night was randomly selected in each subject and used to carry out the test of interest (e.g., unpaired t-test). Ultimately, the test was considered statistically significant when it yielded a significant effect in more than 95% of iterations ( $\alpha = 0.05$ ). For topographic (channel-by-channel) comparisons, correction for multiple comparisons was performed at each iteration by using a permutation-based supra-threshold cluster correction, as described in previous work (33) (9). In brief, the same comparison (or correlation) was repeated (1,000 repetitions) after shuffling the labels of the two groups (or values of one

variable, for correlations) and the maximum size of significant electrode-clusters ( $p < 0.05$ ;  $|t_{(30)}| > 2.04$  for comparisons and  $|r_{(47)}| > 0.28$  for correlations) was saved in a frequency table. A minimum cluster-size threshold corresponding to the 95th percentile of the resulting distribution was applied to correct for multiple comparisons. In summary, each topographic analysis included 1 million iterations: 1,000 for randomization of the nights used in the test, and 1,000 for the definition of the significance threshold in each step of the permutation procedure. T-score values (or r-values, for correlations) displayed in color maps of topographic analyses were obtained by performing the specific test of interest after averaging available nights for each subject. Analyses were performed in MATLAB (Matlab, The Math Works Inc, Natick, MA).

## ***Results***

### *Definition of the falling asleep period*

To verify that the falling asleep period, which was defined by visual inspection here, was comparable between adults and children, we calculated the variation in delta (SWA) and alpha spectral power in the first epoch of the falling asleep period relative to the preceding (pre-sleep) 30-sec period (corresponding here to 100% value) for each subject. Alpha activity decreased significantly ( $p < 0.0001$ ) after the visually marked 'EA' event in both children ( $54.55 \pm 17.23$  %, relative to pre-sleep period) and young adults ( $46.92 \pm 23.73$  %). Delta activity significantly increased ( $124.37 \pm 18.12$  % and  $124.99 \pm 30.82$  %) in both groups ( $p < 0.0001$ ) immediately after the EA event. Of note, no differences in relative changes (30s before the EA vs 30s after the EA) emerged between groups (alpha,  $p > 0.23$ ; delta,  $p > 0.95$ ), indicating that the beginning of the falling asleep period was consistently defined across groups.

### *Duration of the falling asleep period and polysomnographic parameters*

Duration of the falling asleep periods and polysomnographic parameters for children and adults are shown in Supplementary table 1. Children took longer to reach sleep stage N2 after lights-off (sleep latency), but showed a faster progression from the end of

wakefulness to stable sleep (end of alpha to first slow wave sequence). Children displayed significantly longer total recording times, lower sleep efficiency, longer wake after sleep onset, a higher proportion of N1 and a lower proportion of REM sleep. There was also a non-significant trend towards more N3 sleep and longer total sleep times in children. These differences may suggest that young adults in this group were slightly more ‘sleep deprived’. Alternatively, this may indicate that young adults were less influenced by the laboratory setting and therefore ‘slept better’. Indeed, most of the ‘young adults’ were included in the study by Fattinger et al. (24), in which subjects underwent a very strict selection procedure (after the screening/adaptation night, only subjects who slept very well were included). Major sleep deprivation seems however unlikely given that actigraphy was performed prior to the recording to monitor bed and rise times, and the proportion of N3 sleep, a good structural marker of the effects of sleep deprivation, is clearly in the normal range for this age group.

#### *Changes in slow wave characteristics in the course of the falling asleep period*

Next, we studied how slow wave parameters changed in the course of the falling asleep process (Fig. 2) in both children (age 8-11) and young adults (age 20-25). As expected, in both groups, the overall number, amplitude and slope of slow waves increased in the course of the falling asleep period (Fig. 2, Fig. S1). Examples of the EEG signal in children and young adults for early and late epochs of the falling asleep period are shown in Fig. 3. In children, the density, amplitude and slope increased almost linearly and in parallel in all ROIs (*‘child pattern’*, Fig. 2B and 4A) from the beginning to the end of the falling asleep period, while in young adults, the same parameters displayed intersecting and temporally dissociated courses (*‘adult pattern’*, Fig. 2C and 4B), similar to those recently described in older adults. More specifically, in young adults, slow wave density increased slowly at the beginning and rapidly at the end of the falling-asleep process, while slow wave amplitude and slope increased most rapidly initially, reaching their maximum around epoch 6 before starting to decrease. At the very end of the falling asleep period (epoch 10), slow wave amplitude started to increase again in this group (6). The maximal dissociation between slow wave amplitude and density in young adults was observed in the anterior medial ROI (Fig 2C). Therefore, representative examples of

individual subjects are shown in the lower panels of Figure 4 for this region. The distinct ‘child’ and ‘adult’ patterns were also obtained by applying different slow wave amplitude thresholds (80, 100 or 120  $\mu\text{V}$  instead of 40  $\mu\text{V}$ ) and including slow waves with a broader duration (0.1-1.0 sec, instead of 0.25-1.0 sec; data not shown), indicating that these results are not threshold-dependent. Given that amplitude and slope were highly correlated and showed similar changes during the falling asleep process, further analyses were restricted to slow wave amplitude only, in addition to slow wave density.

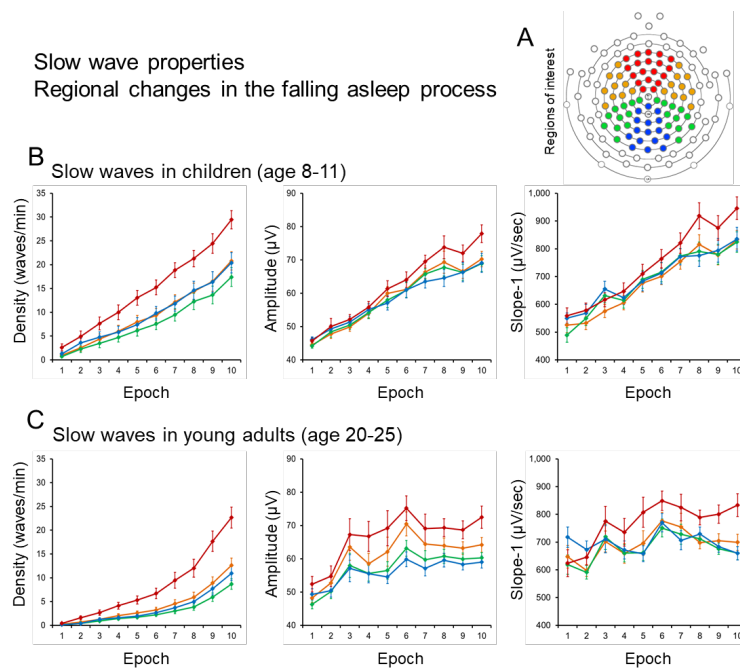
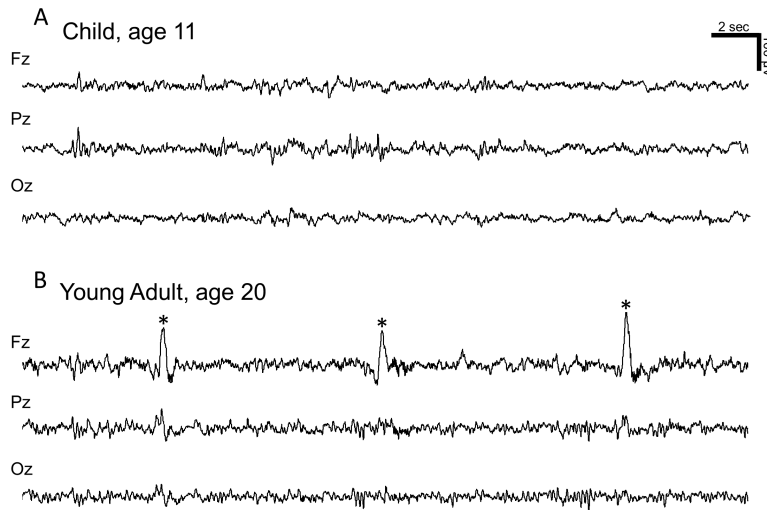


*Fig. 2. Regional changes in slow wave properties across the falling asleep process. Slow wave density (slow waves/min, first column), amplitude ( $\mu\text{V}$ , second column) and slope (positive to negative deflection,  $\mu\text{V}/\text{sec}$ , third column) over the 10 epochs of the falling asleep period for each region of interest in children (B, age 8 to 11) and young adults (C, age 20 to 25). Regions of interest are shown in panel A: medial anterior (dark red), lateral anterior (orange), medial posterior (blue), lateral posterior (green).*

**Representative EEG traces in early epochs**



**Representative EEG traces in late epochs**

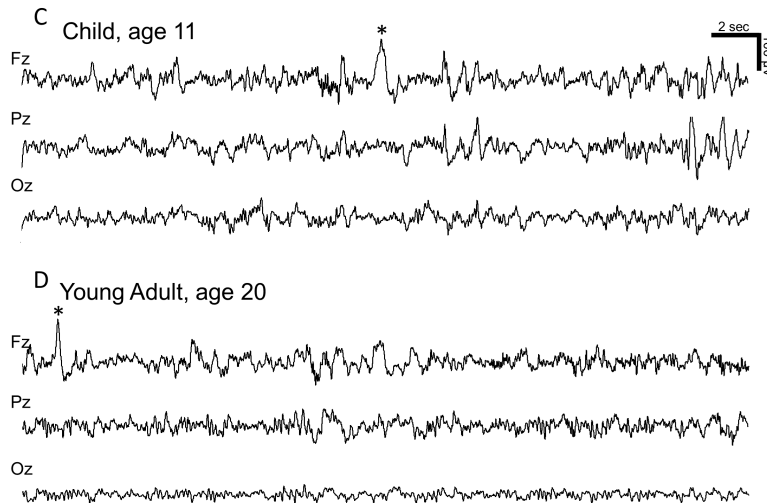


*Fig. 3. Representative EEG traces in early and late epochs. (A-B) Representative examples of EEG traces for selected frontal (Fz), parietal (Pz) and occipital (Oz) electrodes in early epochs of a child (A, age 11) and of a young adult subject (B, age 20). (C-D) Representative examples of EEG traces in late epochs of a child (C, age 11) and of a young adult (D, age 20). Asterisks (\*) mark potential type I slow waves.*

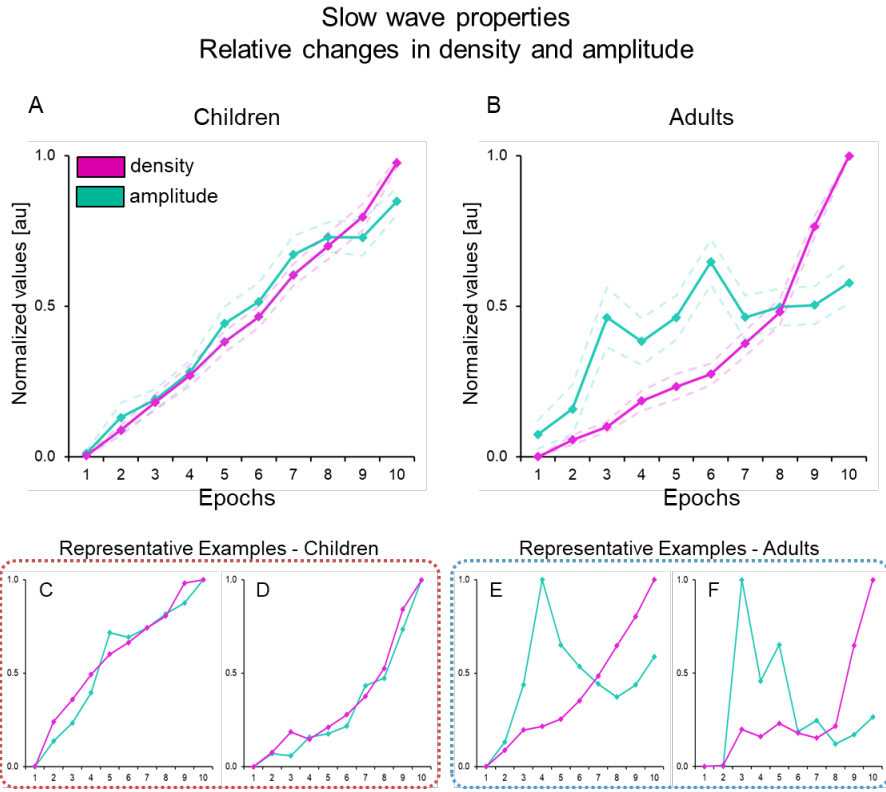


*Fig. 4. Changes in slow wave density and amplitude in the falling asleep process. Changes in slow wave density (pink) and amplitude (cyan) in the medial anterior region over the 10 epochs of equal length in children (A, age 8 to 11) and young adults (B, age 20 to 25). The medial anterior region is shown because it displayed markedly dissociated temporal courses for slow wave amplitude and density in adults (see Fig. 2). For each subject, values were re-scaled between 0 and 1. Dashed lines indicate the standard error. The lower panels display individual representative examples from children aged 9.56 (C) and 11.1 (D) and young adults aged 20.38 (E) and 23.56 (F).*

#### *Topographical changes in slow wave characteristics*

Both in early (2-3) and late (8-9) epochs of the falling asleep process, children showed a higher slow wave density in central and posterior electrodes relative to young adults (Fig 5A), and these parameters negatively correlated with age in the same regions (Fig. S2A). Slow wave amplitude, on the other hand, was significantly higher in adults in frontal areas in earlier epochs (Fig 5A) and positively correlated with age in these regions (Fig. S2A). This is consistent with findings presented in Fig. 4, indicating the presence of high-

amplitude slow waves in the first phase of the falling asleep period in young adults but not in children. In late epochs, slow wave amplitude was higher in centro-posterior areas in children compared to adults (Fig 5A) and negatively correlated with age (Fig. S2A), but these analyses did not reach statistical significance. Slow wave density and amplitude increases over the 10 time epochs of equal length were greater in children compared to young adults in posterior and central brain regions, respectively (Fig. 5B and Fig. S2B). Next, we quantified the speed of slow wave density and amplitude changes over absolute time in children and adults. Here again, compared to young adults, children displayed faster slow wave density and amplitude increases in posterior and central brain regions, respectively (Fig. 6). The speed of increase of these parameters in the course of the falling asleep period also negatively correlated with age (Fig. S3). It should be noted that although the average slow wave amplitude in children was lower in early epochs than that observed in young adults, upon visual inspection, some individual slow waves appeared to be just as large as those observed in adults in this phase of the falling asleep process. Indeed, an additional analysis comparing ‘the single largest’ slow wave of each participant between adults and children showed only a weakly significant trend towards a higher slow wave amplitude in adults in a frontal electrode, while no differences were observed in occipital and parietal channels (Fig. 7).

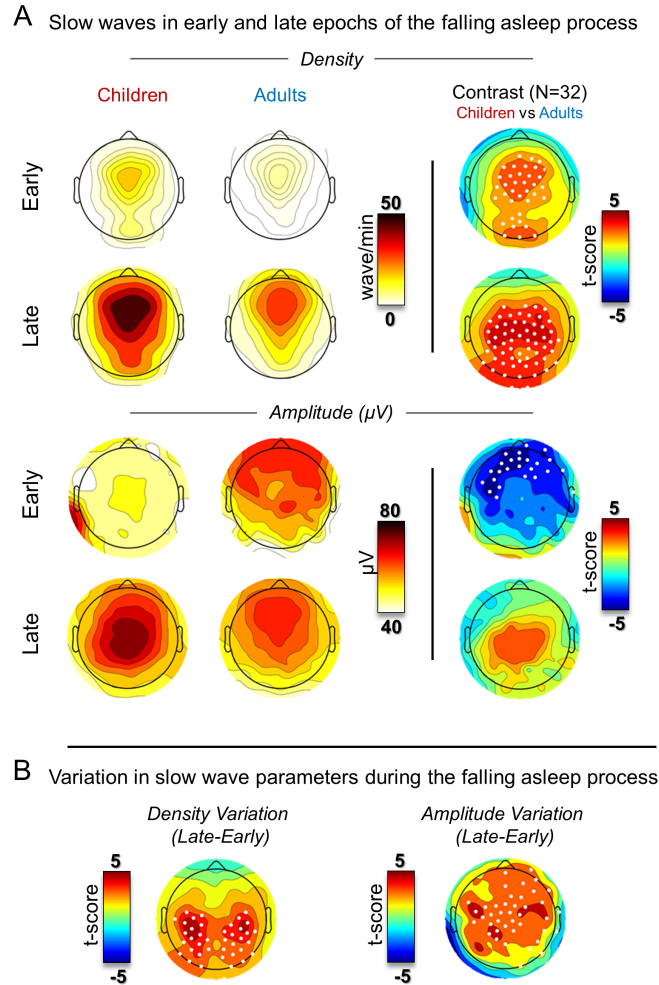


*Fig. 5. Topographic distribution of slow wave properties in early and late epochs of the falling asleep process. (A) Absolute values of slow wave density (slow waves/min) and amplitude ( $\mu V$ ) in children (first column) and adults (second column) during early (2-3) and late (8-9) epochs of the falling asleep process. The third column shows the statistical contrast between children,  $N=16$ , and adults,  $N=16$ . White dots indicate statistically significant results ( $p < 0.05$ , cluster-size-based correction). The red color indicates higher values in children/younger subjects, the blue color higher values in adults/older subjects. (B) Differences in slow wave parameter changes (density, left; amplitude, right) between children and adults in the falling asleep process (i.e., from early to late epochs). White dots indicate statistically significant results ( $p < 0.05$ , cluster-size-based correction). The red color reflects a larger increase in slow wave density or amplitude between early and late epochs in younger subjects.*

### Speed of density and amplitude changes

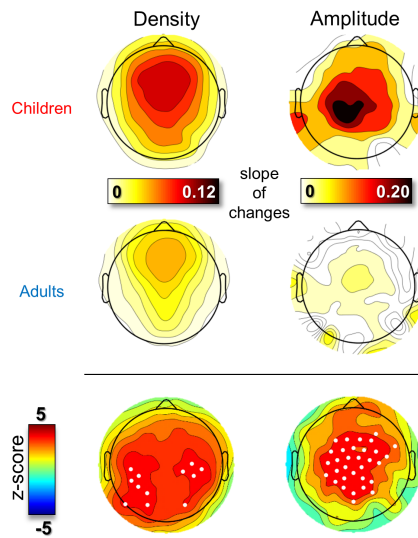


Fig. 6. *Topographic distribution of the speed of changes in slow wave density (left column) and amplitude (right column) in the course of the falling asleep process (across absolute time starting at the end-of-alpha activity) in children (first row) and adults (second row). The last row shows the results of the statistical contrast between children and adults (non-parametric permutation test with cluster-size-based correction for multiple comparisons). Here the red color indicates a faster density/amplitude increase in children relative to adults.*

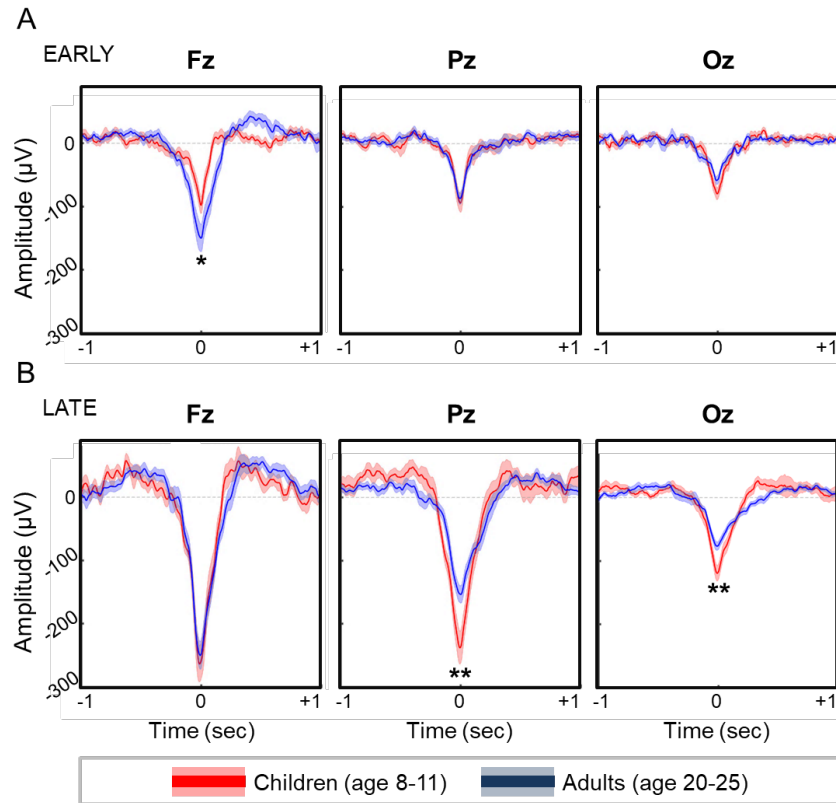
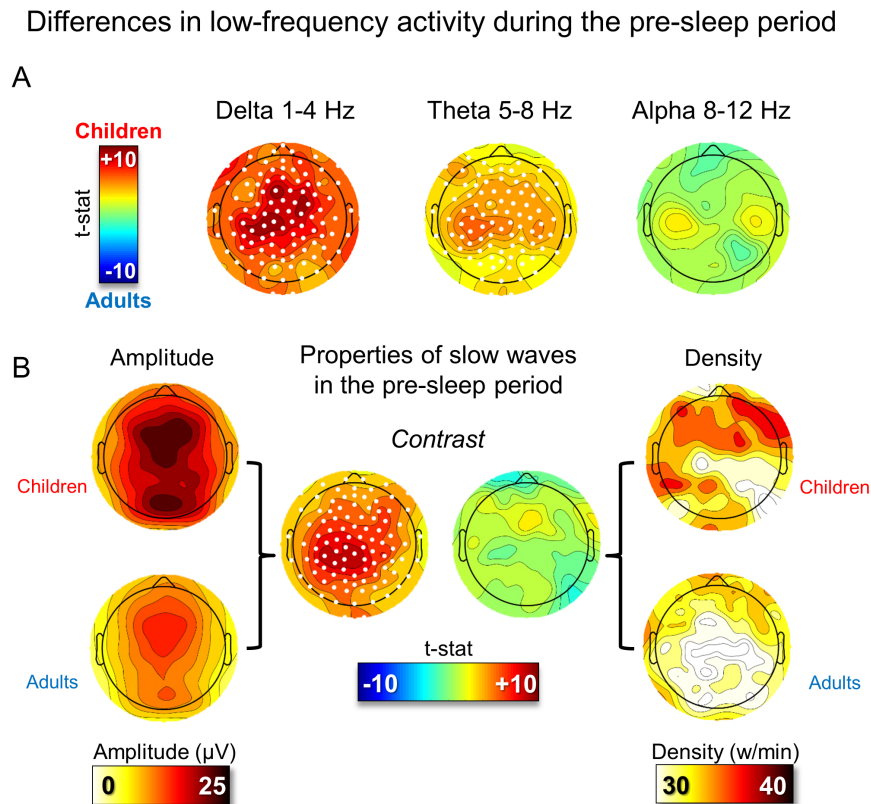


Fig. 7. Amplitude of the single largest slow waves detected in early (A) and late (B) epochs of the falling asleep process in children (red) and young adults (blue). Three representative channels are shown: Fz, Pz, Oz. \*  $p < 0.05$  uncorrected, \*\*  $p < 0.05$  Bonferroni corrected (based on the number of tested electrodes).

#### Brain activity during wakefulness immediately prior to sleep

During the 30 seconds of wakefulness preceding the first stage of sleep, children displayed significantly higher delta (1-4 Hz) and theta (4-8 Hz) power than the young adults ( $p < 0.05$ , cluster-size-based correction; Fig. 8A). An additional analysis comparing the amplitude and density of slow waves between the two age groups in pre-sleep wakefulness showed that the higher power values in children resulted mainly from a larger slow wave amplitude in this age group (rather than from a greater number of slow waves) (Fig. 8B). Finally, as shown in Fig. S4, in adults, a significant correlation between pre-sleep delta power and the speed of increase in slow wave density was observed in all ROIs. A similar effect was observed for theta in the lateral posterior region. A positive

but weaker and non-significant correlation was observed in children. Neither adults nor children showed a correlation between pre-sleep delta or theta and the speed of increase in slow wave amplitude.



*Fig. 8. Differences in SWA and slow waves during wakefulness immediately prior to sleep (30 sec before end of alpha). (A) Differences in power spectral density for the delta, theta, and alpha bands between children and young adults (white dots;  $p < 0.05$ , cluster-size-based correction). (B) Differences in slow wave density (right) and amplitude (left) between children and young adults. The central section of the figure shows significant differences (white dots;  $p < 0.05$ , cluster-size-based correction).*

## **Discussion**

Slow waves in the falling asleep period displayed several differences in children with respect to young adults: i) slow wave number and amplitude increased linearly and in parallel as opposed to the dissociated, intersecting courses seen in adults, ii) slow waves were larger and more numerous in central and posterior brain regions, respectively, and the younger the child, the faster these parameters increased in these areas during the falling asleep period, iii) slow waves in children were larger in almost all cortical regions during pre-sleep wakefulness, with a maximum in central brain areas.

### *Slow wave synchronization processes*

In young adults, slow wave density and amplitude followed dissociated, intersecting courses: slow wave density increased slowly at the beginning and rapidly at the end of the falling-asleep period, while slow wave amplitude and slope increased most rapidly initially and then decreased before increasing again at the very end of the falling asleep period. This dissociation indicates that in adults, at the beginning of the falling asleep period, large, steep and isolated slow waves prevail, while towards stable sleep, numerous smaller slow waves, which progressively increase in amplitude become the predominant feature. These findings confirm results from a previous study performed in older adults (6), who displayed the same dissociation between slow wave density and amplitude at sleep onset. Studies using large-scale computer simulations (34), local field potentials in rats (35) and EEG in humans (29) suggest that slow wave amplitude reflects the number of neurons that simultaneously enter a hyperpolarized down-state, while the first slope of slow waves relates to the speed at which this synchronized down-state is reached. Thus, slow waves with steep slopes and large amplitudes result from a rapid and efficient neuronal synchronization of a large number of neuronal populations. The fact that characteristics of early slow waves differ from late slow waves suggests that two separate slow wave synchronization mechanisms sequentially come into play at sleep onset: a strong and efficient synchronization process (synchronization process I) producing large and steep slow waves (which we call ‘type I slow waves’, and which likely include slow waves traditionally referred to as ‘K-complexes’) followed by a

weaker synchronization process (synchronization process II) giving rise to smaller and shallower slow waves (which we call ‘type II slow waves’, and which likely include slow waves traditionally referred to as ‘delta waves’) (6). Source modeling analyses performed in a previous study revealed that early slow waves (‘type I’) preferentially originated in sensorimotor regions and the posterior-medial parietal cortex and involved broad fronto-central regions, while late slow waves (‘type II’) could originate anywhere in the cortex and tended to involve more circumscribed cortical areas (6). In addition, several lines of evidence suggest that synchronization process I is related to arousal systems while synchronization process II is not: early slow waves originate in regions that display the highest noradrenergic innervation in the human and monkey cortex (36-38) and are typically followed by ‘EEG activations’ (39). In addition, neuroimaging studies have shown that very large amplitude slow waves are specifically associated with brainstem activations including the locus coeruleus (40). It is thus likely that synchronization process I operates in a bottom-up manner (subcortico-cortical), through diffuse projections of arousal systems (41-43), reaching many fronto-central regions of the cortex at the same time, which explains the broad frontal involvement and the strong synchronization underlying characteristics of type I slow waves. Synchronization process II, on the other hand, is likely to be cortico-cortical, reaching few neurons at the same time, which would account for the circumscribed cortical involvement and other features of type II slow waves.

The parallel and linear increase of slow wave amplitude and number in children suggests that the two synchronization processes are not temporally dissociated in the falling asleep period in children. The distinct ‘child-pattern’ was also observed when increasing slow wave amplitude thresholds were applied, suggesting that it is not due to the fact that larger type II slow waves in children ‘mask’ potential type I slow waves. Instead, the first phase of the falling asleep period, characterized by isolated, large amplitude (type I) slow waves, seems to be truly missing in children. Consistent with this, in early epochs of the falling asleep period, children displayed smaller slow waves compared to adults (Fig. 5). This is relatively surprising, given that large-amplitude slow waves (so-called ‘K-complexes’) are known to occur in children from the age of 5 to 6 months onwards (44,

45), either spontaneously or in response to sensory stimulation. In addition, children sometimes present hypersynchronous, large-amplitude waves in the theta and delta range at sleep onset and upon awakening (45, 46). Visual inspection of the raw EEG traces in the course of the falling asleep period revealed indeed the presence of large, steep fronto-central slow waves, comprising slow waves that are traditionally referred to as K-complexes, also in children. However, instead of appearing on a relatively flat ('desynchronized') EEG background like in adults, these elements occurred on a background of much slower activity in the theta-delta frequency range, likely comprising type II slow waves (see for example Fig. 3C). In addition, visual inspection and quantitative analyses showed that the largest slow waves in children in early phases of the falling asleep period tended to be just as large and widespread as typical early slow waves in adults (Fig. 7), suggesting that at least most of these slow waves represent type I slow waves in children. It is thus likely that both slow wave synchronization processes are already present in children. However, they do not display the temporal segregation that is typically seen in the falling asleep period in adults. What could account for the absence of the temporal dissociation of the two processes in children?

One possibility is that synchronization process II starts earlier in children, at the expense of synchronization process I. Recent work in adults has shown that the two types of slow waves have different effects on one another (39) type I slow waves, for instance, tend to be smaller when they occur immediately after a type II slow wave than when they occur in isolation. This might be a result of regional de-synchronization, when different brain areas are giving rise to small, local (type II) slow waves, which interfere with the synchronization of widespread oscillations (type I slow waves). It is thus conceivable that an earlier start of synchronization process II in children may in this way interfere with the synchronization of type I slow waves in this phase of sleep. If this were the case, the first phase of sleep in children would be much like stable slow wave sleep in adults, consisting of many type II slow waves and reduced amplitude type I slow waves (39). One could ask here if this earlier start of synchronization process II is due to the fact that children might be more 'sleep deprived' than adults. This is however unlikely, given that children were allowed to go to bed at their usual bedtime, and adherence to regular sleep schedules in

the week prior to the study was verified by actigraphy. In addition, the dissociation between the two synchronization processes at sleep onset was previously documented in adults in conditions of strong sleep fragmentation/restriction, suggesting that it persists even in the face of globally elevated homeostatic sleep pressure (6). However, it is conceivable that children display a ‘locally’ increased propensity to generate slow waves, in relation with age-related maturation of specific cortical regions, and a faster build-up of sleep pressure (47), which could lead to a fast and linear increase of type II slow waves after sleep onset and interfere with the synchronization of type I slow waves. Consistent with this interpretation, we found that children, compared to young adults, displayed more slow waves posteriorly and larger slow waves in central brain regions in the late parts of the falling asleep period. In addition, the younger the subject, the faster slow wave amplitude and number increased in the course of the falling asleep period in central and posterior regions, respectively (Fig. 6). These findings are in line with previous work showing that the SWA maximum during NREM sleep is confined to posterior brain regions before age 8, then progressively includes central brain regions (age 8-14) before it shifts to anterior cortical areas (after age 14) (17). SWA in childhood has been shown to mirror the development of regionally specific skills (11, 20) and age-dependent decreases in cortical grey matter (19), suggesting that it reflects changes in cortical plasticity related to brain maturation (19, 48), including synaptic pruning and/or reorganization (22). Our results extend these findings to the falling asleep period, by showing that not only slow waves are larger and more numerous in central and posterior regions in younger children, respectively, but also that these maturing regions ‘fall asleep faster’, possibly as a result of an increased propensity to generate local slow waves in the context of plasticity-related cortical processes. It is tempting to speculate that the predominance of slow waves in posterior and particularly in sensory regions in children during the falling asleep period and beyond may account for the high resistance to awakenings induced by sensory stimulations (49). Indeed, children are not only hard to awaken, but when they do, may display behavioral manifestations of incomplete and ‘dissociated’ awakenings, such as confusional arousals, somnambulism (NREM parasomnias) or extreme sleep inertia (50, 51), which are rather exceptionally observed in adults. Future studies should address whether the superposition of arousal- (type I) and

sleep promoting processes (type II) early in the night may explain frequent sleep-related behaviors in children, like arousal disorders. The observation that children display more SWA in maturing parieto-occipital regions compared to adults may explain why dream frequency is reduced in children as opposed to adults (52). In fact, recent work has shown that increases in SWA over parieto-occipital brain regions are associated with unconsciousness during sleep, while local decreases of SWA in these areas predict the presence of dreaming (53). While the most dramatic increases in dream frequency occur between age 5 and 9 (for both REM and NREM sleep), after age 9, further increases in NREM dreaming are seen specifically during slow wave sleep early in the night (52), consistent with our results and the progressive posterior-anterior shift of the SWA maximum in this age group.

#### *Slow waves during pre-sleep wakefulness in children*

Finally, we found that compared to young adults, children displayed larger slow waves in the wake period immediately preceding sleep onset, especially in central brain areas. Slow oscillations during wakefulness have been documented in both humans and animals, especially during sleep deprivation (30) (31), and have been hypothesized to represent 'local sleep in wakefulness'. Contrary to adults, in children we did not find a significant correlation between delta power during wakefulness immediately prior to sleep and the speed of the falling asleep process. The absence of correlation is not clear but could be due to the fact that delta power reached a 'ceiling effect' in this population. A previous study, in which adults were kept awake for extended periods of time and had to perform a frontal executive task battery (32), documented a temporal association between the occurrence of frontal and parietal slow waves during wakefulness and impulse control errors. It would be insightful to study how the occurrence of these slow waves shortly before sleep onset relate to failures in self-regulation, including motor hyperactivity and difficulties with impulse control, which are sometimes seen in younger children at bedtime. Consistent with our results, a recent study performed in children showed that theta waves became more widespread in the evening compared to the morning, and were associated with a performance decline in an attention task (54-56). This tendency to

display more ‘local sleep in wakefulness’ in the transition to sleep in children may be due to a faster build-up of homeostatic sleep pressure at this age (47).

### *Limitations*

Because the two synchronization processes do not appear to be temporally dissociated in children, we could not directly compare characteristics of potential ‘type I’ (early) and ‘type II’ (late) slow waves between the two age groups, and verify our hypothesis that only type II slow waves show age-dependent regional changes. Future studies, using classification approaches that allow to distinguish type I and type II slow waves independently of their temporal occurrence in the sleep-wake transition will allow to verify this hypothesis more directly.

Our approach used for analysis of the falling asleep segments is based on the assumption that the falling asleep period is a process, ranging from the EA to the FSS irrespective of the duration of the interval between these two events. Compared to an approach based on a fixed time point to define sleep onset (i.e. the first sleep spindle (3, 57, 58)), this approach is better suited to capture the gradual regional changes that occur in this period. In addition, it allows to compare falling asleep periods of different lengths (5, 59, 60) and accounts for the fact that the falling asleep process can occur rapidly or slowly (depending on sleep pressure).

It should be mentioned that this study was performed retrospectively, on hd-EEG recordings that were not specifically acquired to study the falling asleep period. To include a sufficient number of subjects within the two age ranges, recordings were pooled from three different studies. As a consequence, because of the different study protocols, some subjects underwent cognitive testing, visuo-motor tasks and TMS sessions prior to the recordings. Although we cannot exclude that these interventions may have influenced the topography of slow waves, it is unlikely that they significantly modified the course of slow waves in the falling asleep period. In addition, our permutation-based statistic was designed to control for the effect of different study nights.

Finally, the falling-asleep epochs that were analyzed represent selected episodes, free of artifacts and major arousals, and may therefore not be fully representative of physiological wake-sleep transitions. This selection enabled us to keep recording segments as a whole, without discarding any parts, and this was necessary in order to compare falling-asleep periods of different lengths. It is possible that the selection of very continuous transitions may have favored the preferential inclusion of subjects with relatively high sleep pressure. However, it is unlikely that this fundamentally affected our results, given that indications for sleep deprivation were excluded by actigraphy prior to the recording, and the dissociation of the two synchronization processes was equally documented previously in conditions of strong sleep restriction/deprivation (6).

### *Conclusions*

In conclusion, our results indicate that the temporal dissociation of the two slow wave synchronization processes observed in adults in the falling asleep period is not yet present in young children. Whether the superposition of arousal- and sleep promoting processes early in the night may explain frequent sleep-related behaviors in children, like arousal disorders, needs to be determined by future studies. Our study also shows that maturing posterior and central brain regions fall asleep ‘faster’ compared to adults. Finally, children display larger slow waves during wakefulness immediately prior to sleep, with potential implications for behavior at bedtime.

### **Acknowledgements**

This work was supported by the Swiss National Science Foundation Grants PZ00P3\_173955 (F.S.), PP00A3-114923 (R.H.), PP00P3-135438 (R.H.) and 320030\_153387 (R.H.), the Clinical Research Priority Program ‘Sleep and Health’ of the University of Zürich (R.H.), the Zürich Center for Integrative Human Physiology (ZHIP) (R.H.), the Anna Mueller Grocholski Foundation (R.H.), the Divesa Foundation Switzerland (F.S.), the Pierre-Mercier Foundation for Science (F.S.), the Bourse Pro-Femme of the University of Lausanne (F.S.), and an EMBO short-term postdoctoral fellowship (G.B.).

## References

1. Siclari F, Larocque JJ, Postle BR, Tononi G. Assessing sleep consciousness within subjects using a serial awakening paradigm. *Front Psychol.* 2013;4:542.
2. Siclari F, Tononi G. Local aspects of sleep and wakefulness. *Curr Opin Neurobiol.* 2017;44:222-7.
3. Sarasso S, Proserpio P, Pigorini A, Moroni F, Ferrara M, De Gennaro L, et al. Hippocampal sleep spindles preceding neocortical sleep onset in humans. *Neuroimage.* 2013.
4. Magnin M, Rey M, Bastuji H, Guillemant P, Mauguire F, Garcia-Larrea L. Thalamic deactivation at sleep onset precedes that of the cerebral cortex in humans. *Proc Natl Acad Sci U S A.* 2010;107(8):3829-33.
5. Marzano C, Moroni F, Gorgoni M, Nobili L, Ferrara M, De Gennaro L. How we fall asleep: regional and temporal differences in electroencephalographic synchronization at sleep onset. *Sleep Med.* 2013;14(11):1112-22.
6. Siclari F, Bernardi G, Riedner B, LaRocque J, Benca MR, Tononi G. Two distinct synchronization processes in the transition to sleep: a high-density electroencephalographic study. *Sleep.* 2014;37(10):1621-37.
7. Steriade M, Timofeev I, Grenier F. Natural waking and sleep states: a view from inside neocortical neurons. *J Neurophysiol.* 2001;85(5):1969-85.
8. Achermann P, Borbely AA. Mathematical models of sleep regulation. *Front Biosci.* 2003;8:s683-93.

9. Huber R, Ghilardi MF, Massimini M, Ferrarelli F, Riedner BA, Peterson MJ, et al. Arm immobilization causes cortical plastic changes and locally decreases sleep slow wave activity. *Nat Neurosci.* 2006;9(9):1169-76.
10. Huber R, Ghilardi MF, Massimini M, Tononi G. Local sleep and learning. *Nature.* 2004;430(6995):78-81.
11. Wilhelm I, Kurth S, Ringli M, Mouthon AL, Buchmann A, Geiger A, et al. Sleep slow-wave activity reveals developmental changes in experience-dependent plasticity. *J Neurosci.* 2014;34(37):12568-75.
12. Feinberg I. Schizophrenia: caused by a fault in programmed synaptic elimination during adolescence? *J Psychiatr Res.* 1982;17(4):319-34.
13. Gaudreau H, Carrier J, Montplaisir J. Age-related modifications of NREM sleep EEG: from childhood to middle age. *J Sleep Res.* 2001;10(3):165-72.
14. Campbell IG, Feinberg I. Longitudinal trajectories of non-rapid eye movement delta and theta EEG as indicators of adolescent brain maturation. *Proc Natl Acad Sci U S A.* 2009;106(13):5177-80.
15. Jenni OG, Borbely AA, Achermann P. Development of the nocturnal sleep electroencephalogram in human infants. *Am J Physiol Regul Integr Comp Physiol.* 2004;286(3):R528-38.
16. Feinberg I, Campbell IG. Sleep EEG changes during adolescence: an index of a fundamental brain reorganization. *Brain Cogn.* 2010;72(1):56-65.
17. Kurth S, Ringli M, Geiger A, LeBourgeois M, Jenni OG, Huber R. Mapping of cortical activity in the first two decades of life: a high-density sleep electroencephalogram study. *J Neurosci.* 2010;30(40):13211-9.

18. Shaw P, Kabani NJ, Lerch JP, Eckstrand K, Lenroot R, Gogtay N, et al. Neurodevelopmental trajectories of the human cerebral cortex. *J Neurosci.* 2008;28(14):3586-94.
19. Buchmann A, Ringli M, Kurth S, Schaerer M, Geiger A, Jenni OG, et al. EEG sleep slow-wave activity as a mirror of cortical maturation. *Cereb Cortex.* 2011;21(3):607-15.
20. Kurth S, Ringli M, Lebourgeois MK, Geiger A, Buchmann A, Jenni OG, et al. Mapping the electrophysiological marker of sleep depth reveals skill maturation in children and adolescents. *Neuroimage.* 2012;63(2):959-65.
21. Tononi G, Cirelli C. Sleep and the price of plasticity: from synaptic and cellular homeostasis to memory consolidation and integration. *Neuron.* 2014;81(1):12-34.
22. Hoel EP, Albantakis L, Cirelli C, Tononi G. Synaptic refinement during development and its effect on slow-wave activity: a computational study. *J Neurophysiol.* 2016;115(4):2199-213.
23. de Vivo L, Faraguna U, Nelson AB, Pfister-Genskow M, Klapperich ME, Tononi G, et al. Developmental patterns of sleep slow wave activity and synaptic density in adolescent mice. *Sleep.* 2014;37(4):689-700, A-B.
24. Fattinger S, de Beukelaar TT, Ruddy KL, Volk C, Heyse NC, Herbst JA, et al. Deep sleep maintains learning efficiency of the human brain. *Nat Commun.* 2017;8:15405.
25. Wehrle FM, Latal B, O'Gorman RL, Hagmann CF, Huber R. Sleep EEG maps the functional neuroanatomy of executive processes in adolescents born very preterm. *Cortex.* 2017;86:11-21.

26. Iber C, Ancoli-Israel S, Chesson A, Quan SF. The AASM Manual for the Scoring of Sleep and Associated Events: Rules, Terminology and Technical Specifications. 1st ed. Westchester, Illinois: American Academy of Sleep Medicine; 2007.
27. Ogilvie RD. The process of falling asleep. *Sleep Med Rev.* 2001;5(3):247-70.
28. Delorme A, Makeig S. EEGLAB: an open source toolbox for analysis of single-trial EEG dynamics including independent component analysis. *J Neurosci Methods.* 2004;134(1):9-21.
29. Riedner BA, Vyazovskiy VV, Huber R, Massimini M, Esser S, Murphy M, et al. Sleep homeostasis and cortical synchronization: III. A high-density EEG study of sleep slow waves in humans. *Sleep.* 2007;30(12):1643-57.
30. Vyazovskiy VV, Olcese U, Hanlon EC, Nir Y, Cirelli C, Tononi G. Local sleep in awake rats. *Nature.* 2011;472(7344):443-7.
31. Hung CS, Sarasso S, Ferrarelli F, Riedner B, Ghilardi MF, Cirelli C, et al. Local experience-dependent changes in the wake EEG after prolonged wakefulness. *Sleep.* 2013;36(1):59-72.
32. Bernardi G, Siclari F, Yu X, Zennig C, Bellesi M, Ricciardi E, et al. Neural and behavioral correlates of extended training during sleep deprivation in humans: evidence for local, task-specific effects. *J Neurosci.* 2015;35(11):4487-500.
33. Nichols TE, Holmes AP. Nonparametric permutation tests for functional neuroimaging: a primer with examples. *Hum Brain Mapp.* 2002;15(1):1-25.
34. Esser SK, Hill SL, Tononi G. Sleep homeostasis and cortical synchronization: I. Modeling the effects of synaptic strength on sleep slow waves. *Sleep.* 2007;30(12):1617-30.

35. Vyazovskiy VV, Riedner BA, Cirelli C, Tononi G. Sleep homeostasis and cortical synchronization: II. A local field potential study of sleep slow waves in the rat. *Sleep*. 2007;30(12):1631-42.
36. Javoy-Agid F, Scatton B, Ruberg M, L'Heureux R, Cervera P, Raisman R, et al. Distribution of monoaminergic, cholinergic, and GABAergic markers in the human cerebral cortex. *Neuroscience*. 1989;29(2):251-9.
37. Gaspar P, Berger B, Febvret A, Vigny A, Henry JP. Catecholamine innervation of the human cerebral cortex as revealed by comparative immunohistochemistry of tyrosine hydroxylase and dopamine-beta-hydroxylase. *J Comp Neurol*. 1989;279(2):249-71.
38. Lewis DA, Morrison JH. Noradrenergic innervation of monkey prefrontal cortex: a dopamine-beta-hydroxylase immunohistochemical study. *J Comp Neurol*. 1989;282(3):317-30.
39. Bernardi G, Siclari F, Handjaras G, Riedner BA, Tononi G. Local and widespread slow waves in stable NREM sleep: evidence for distinct regulation mechanisms. Submitted. 2018.
40. Dang-Vu TT, Schabus M, Desseilles M, Albouy G, Boly M, Darsaud A, et al. Spontaneous neural activity during human slow wave sleep. *Proc Natl Acad Sci U S A*. 2008;105(39):15160-5.
41. Kuramoto E, Ohno S, Furuta T, Unzai T, Tanaka YR, Hioki H, et al. Ventral Medial Nucleus Neurons Send Thalamocortical Afferents More Widely and More Preferentially to Layer 1 than Neurons of the Ventral Anterior-Ventral Lateral Nuclear Complex in the Rat. *Cereb Cortex*. 2013.

42. Jones EG. The thalamic matrix and thalamocortical synchrony. *Trends Neurosci.* 2001;24(10):595-601.
43. Desbois C, Villanueva L. The organization of lateral ventromedial thalamic connections in the rat: a link for the distribution of nociceptive signals to widespread cortical regions. *Neuroscience.* 2001;102(4):885-98.
44. Fisch BJ. *Fisch and Spehlmann's EEG Primer.* 3 ed: Elsevier; 1999.
45. Kellaway P, Fox BJ. Electroencephalographic diagnosis of cerebral pathology in infants during sleep. I. Rationale, technique, and the characteristic of normal sleep in infants. *J Pediatr.* 1952;41:262-87.
46. Gibbs FA, Gibbs EL. *Atlas of electroencephalography:* Addison-Wesley Publishing Company; 1950.
47. Jenni OG, Achermann P, Carskadon MA. Homeostatic sleep regulation in adolescents. *Sleep.* 2005;28(11):1446-54.
48. Gogtay N, Giedd JN, Lusk L, Hayashi KM, Greenstein D, Vaituzis AC, et al. Dynamic mapping of human cortical development during childhood through early adulthood. *Proc Natl Acad Sci U S A.* 2004;101(21):8174-9.
49. Busby KA, Mercier L, Pivik RT. Ontogenetic variations in auditory arousal threshold during sleep. *Psychophysiology.* 1994;31(2):182-8.
50. American Academy of Sleep Medicine. *International Classification of Sleep Disorders.* American Academy of Sleep Medicine, editor. Darien, IL, 2014.
51. Splaingard M, Hayes J, Smith GA. Impairment of reaction time among children awakened during stage 4 sleep. *Sleep.* 2007;30(1):104-8.

52. Foulkes D. Children's dreaming and the development of consciousness. Cambridge, MA: Harvard University Press; 1999.
53. Siclari F, Baird B, Perogamvros L, Bernardi G, LaRocque J, Riedner B, et al. The neural correlates of dreaming. *Nature Neuroscience*. 2017;20(6):872-8.
54. Fattinger S, Kurth S, Ringli M, Jenni OG, Huber R. Theta waves in children's waking electroencephalogram resemble local aspects of sleep during wakefulness. *Sci Rep*. 2017;7(1):11187.
55. Hagenauer MH, Perryman JI, Lee TM, Carskadon MA. Adolescent changes in the homeostatic and circadian regulation of sleep. *Dev Neurosci*. 2009;31(4):276-84.
56. Carskadon MA, Acebo C, Jenni OG. Regulation of adolescent sleep: implications for behavior. *Ann N Y Acad Sci*. 2004;1021:276-91.
57. Tanaka H, Hayashi M, Hori T. Topographical characteristics of slow wave activities during the transition from wakefulness to sleep. *Clin Neurophysiol*. 2000;111(3):417-27.
58. De Gennaro L, Ferrara M, Curcio G, Cristiani R. Antero-posterior EEG changes during the wakefulness-sleep transition. *Clin Neurophysiol*. 2001;112(10):1901-11.
59. Aeschbach D, Borbely AA. All-night dynamics of the human sleep EEG. *J Sleep Res*. 1993;2(2):70-81.
60. Putilov AA, Donskaya OG. Rapid changes in scores on the two largest principal components of the electroencephalographic spectrum demarcate the boundaries of drowsy sleep. *Sleep and Biol Rhythms*. DOI: 10.1111/sbr.12017.

## Supplementary Text

### *Information on studies from which participants were included*

Most of the subjects included in the analysis (34 subjects and 53 recordings) took part in the study by Kurth et al., 2010 (17) (one night) and Wilhelm et al., 2014 (two nights) (11), in which the authors investigated slow waves characteristics in children of different ages (17) (Kurth et al., 2010) and learning related regional changes in SW activity (11). Before the recordings, one version of a visuo-motor adaptation task, either baseline or adaptation, involving moving a cursor to four possible targets (11) was performed in the evening before going to bed. Three subjects (3 recordings) were control subjects in the study of Wehrle et al (25), which investigated executive functions and SWA in adolescents born preterm. In the afternoon prior to the recordings, subjects underwent an assessment of their IQ, motor and executive function abilities. Twelve subjects (16 recordings) included in the analysis were part of the study of Fattinger et al., (24). The subjects had to perform 12 trials of a 30s “computerized six-element finger sequence tapping task” before going to bed. Because of the short duration of this task, it is unlikely that it caused an impact on the topography of SWA. TMS for a total duration of 5 minutes was also performed to quantify cortical excitability, but again this was very short-lived. In some nights, the subjects were exposed to tones in phase with their slow waves to locally disrupt them. However, this stimulation started later in the night and was not included in the data analyzed in the present study (i.e., the falling asleep process). Of the three studies, one (24) included an adaptation night in addition to two experimental nights, another one (25) included only one experimental night (no adaptation night), and the other one (11, 17) included two experimental nights (no adaptation night). Only experimental nights were included in the analyses: either the first, the second, or both, depending on data quality, the study protocol and availability in the age range.

## Supplementary Figures

### Figure S1

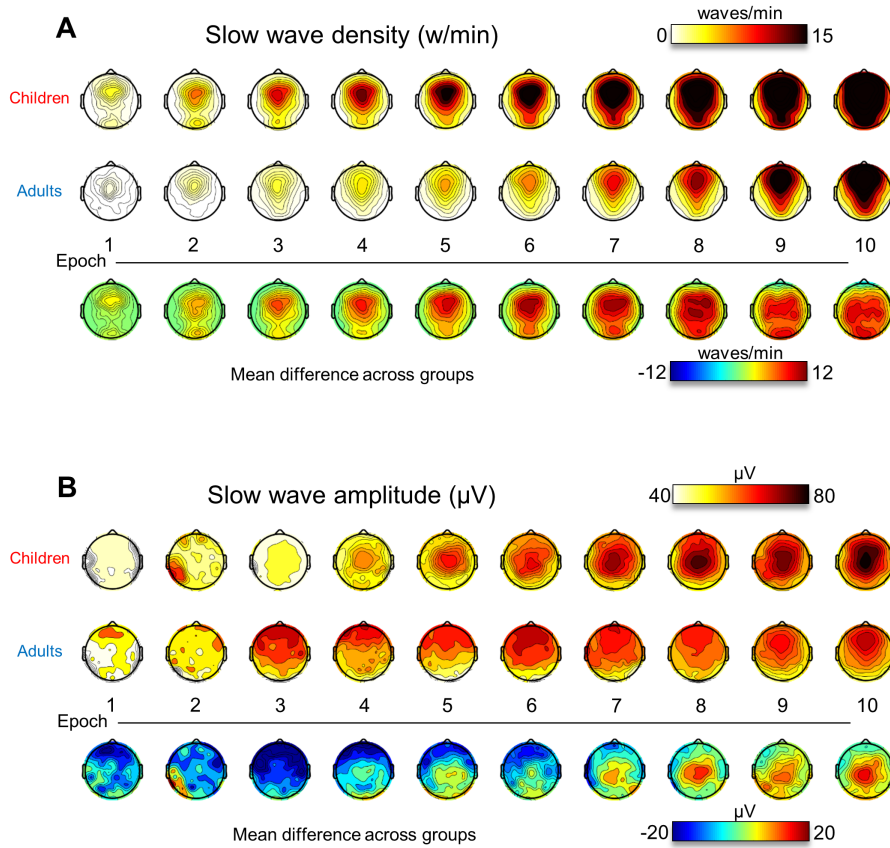


*Fig. S1. Topographic variations in slow wave density (A) and amplitude (B) across ten equal epochs of the falling asleep process, for children (first row) and adults (second row). In each panel, the bottom row shows relative mean differences between the two groups: here the red (blue) color indicates higher values in children (adults).*

Figure S2

Slow waves in early and late epochs of the falling asleep process  
(Correlation analysis between slow wave properties and age, N=49)

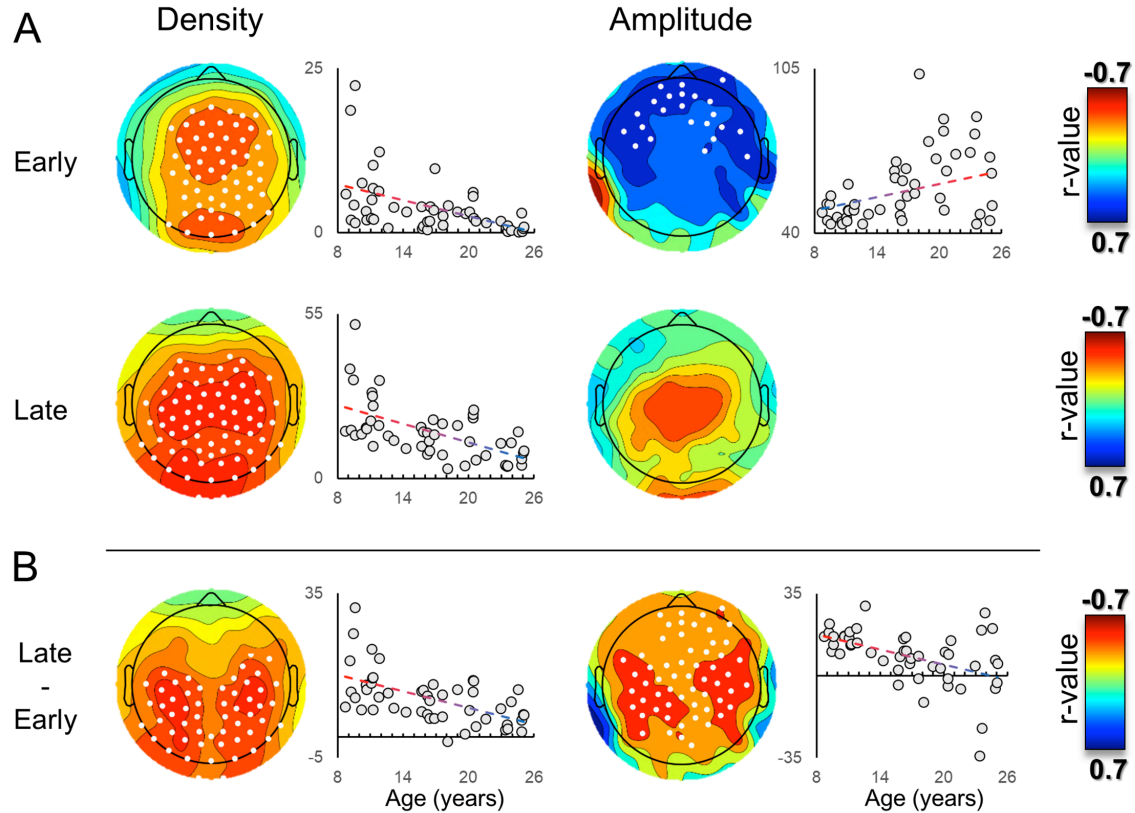
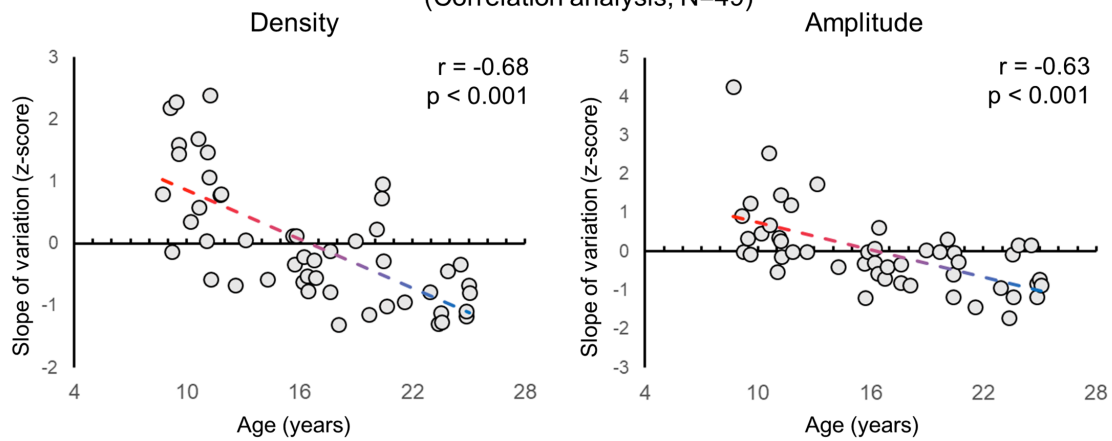


Fig. S2. Age-dependent changes in the topographic distribution of slow wave properties (density, left column; amplitude, right column) across early and late epochs of the falling asleep process (A). Panel B row shows significant differences in relative changes from early to late epochs of the falling asleep period. White dots mark statistically significant correlations (N=49; Pearson's correlation coefficient;  $p < 0.05$ , cluster-size-based correction). Scatterplots display the distribution of individual values as a function of age in electrodes for which the correlation was significant (average). The red color reflects a larger increase in slow wave density or amplitude in younger subjects.

**Figure S3**

**Speed of density and amplitude changes in the falling asleep period**  
(Correlation analysis, N=49)



*Fig. S3. Age-dependent changes in the speed of density (left) and amplitude (right) variations (relative to the absolute time starting from the end-of-alpha activity) in the course of the falling asleep process (N=49, Spearman's correlation coefficient). Younger subjects displayed a faster rate of increase in slow wave density and amplitude. This analysis was performed on the average values of electrodes for which the speed of density and amplitude changes was significantly different between children and adults (Figure 6).*

**Figure S4**

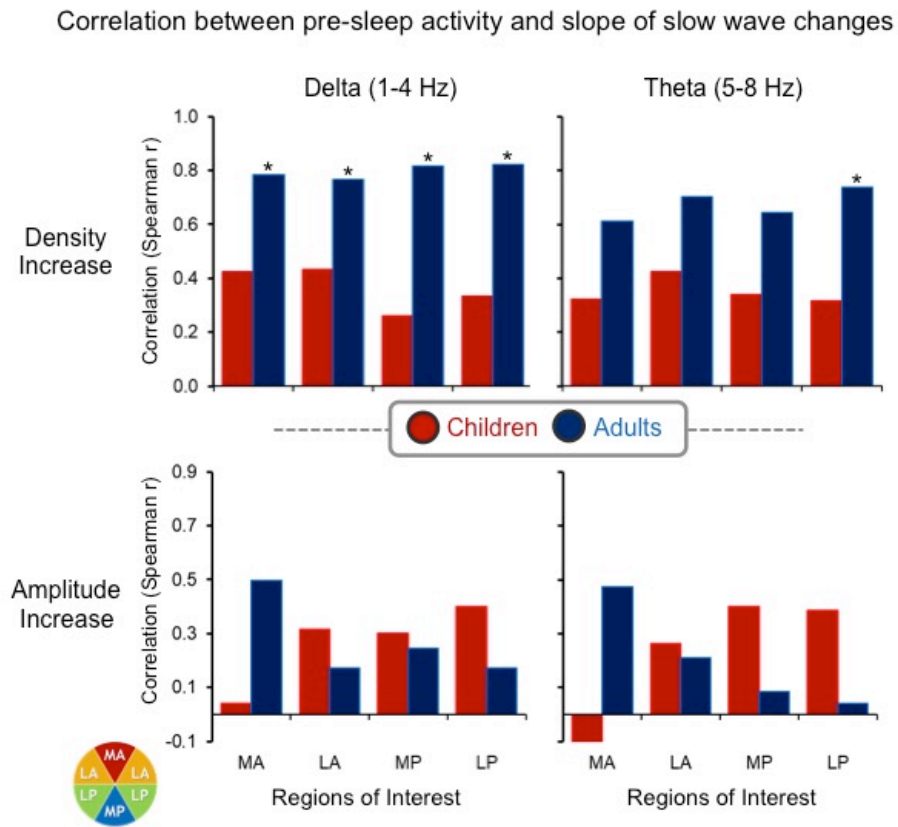


*Fig. S4. Correlation between pre-sleep delta (left)/theta (right) spectral power and the speed of increase in slow wave density (first row)/amplitude (second row), in children (red bars) and adults (blue bars). Significance was tested using a permutation-based approach in which only one night was selected for each subject in each of 1,000 iterations. Effects that resulted significant in more than 95% of the iterations were marked as significant ( $* p < 0.05$ ).*

## Supplementary Table

PSG parameter	Children (age 8-11)	Adults (age 20-25)	P-value
EA-FSS time (min)	10.5 ± 4.8	16.5 ± 4.5	< 0.01
Sleep latency (min)	20.8 ± 6.5	13.2 ± 7.1	< 0.01
Total recording time (min)	506.7 ± 68.9	437.4 ± 24.2	< 0.01
Total sleep time (TST, min)	448.8 ± 73.9	409.8 ± 25.3	0.06
Sleep efficiency (%)	88.2 ± 7.2	93.7 ± 3.3	< 0.01
Wake after sleep onset (min)	40.6 ± 29.4	17.6 ± 10.5	< 0.01
N1 (% TST)	8.3 ± 3.1	5.9 ± 1.9	0.02
N2 (% TST)	48.3 ± 6.2	51.1 ± 6.7	0.22
N3 (% TST)	23.6 ± 7.6	18.6 ± 6.8	0.06
REM (% TST)	19.9 ± 5.2	24.3 ± 3.4	< 0.01

*Supplementary table 1: Polysomnographic (PSG) parameters (mean +/- SD) for children and young adults. Sleep latency is defined here as the time from lights off to the first epoch of stage N2. The EA (End of Alpha activity) – FSS (first sleep sequence) represents the length of the falling asleep process, as defined in the present study. As described in previous work, the EEG was visually scored for sleep stages at frontal, central, and occipital electrodes (20s epochs) based on standard criteria of the American Academy of Sleep Medicine.*